Geochimica et Cosmochimica Acta, 1966, Vol. 30, pp. 9 to 22. Pergamon Press Ltd. Printed in Northern Ireland

Melting relationships in the system CaO–MgO–SiO_2–H_2O at 1 kilobar pressure

G. W. FRANZ[1] and P. J. WYLLIE[2]

[1]Department of Earth Sciences, Southeast Missouri State University
Cape Girardeau, Missouri

[2]Department of the Geophysical Sciences, University of Chicago

(*Received* 17 *June* 1965)

Abstract—Solid–liquid–vapor phase relationships in the system CaO–MgO–SiO_2–H_2O have been determined at 1 kilobar pressure using the quench technique in cold-seal pressure vessels. The phase fields intersected by the composition joins $Ca(OH)_2$–Mg_2SiO_4 and $Ca(OH)_2$–$MgSiO_3$ have been delineated in the temperature range 700–950°C. From these results and from previous work in the bounding systems, a schematic diagram for the phase relationships on the vapor-saturated liquidus surface has been prepared. A thermal divide exists on this surface, corresponding to the melting of mixtures on the join Ca_2SiO_4–MgO in the presence of H_2O vapor. Original liquids with compositions on the SiO_2 side of the divide yield anhydrous crystalline phases and vapor on fractional crystallization, whereas original liquids with compositions on the CaO side of this divide yield hydrated crystalline phases (calciochondrodite and portlandite) plus vapor. The estimated compositions of isobaric invariant liquids at 1 kilobar pressure for the reactions:

portlandite + calciochondrodite + periclase + vapor ⇌ liquid, at 725°C
calciochondrodite + periclase + vapor ⇌ dicalcium silicate + liquid, at 875°C,
are $Ca(OH)_2$–92·7%, Ca_2SiO_4–4·3%, MgO–2·5%, H_2O–0·5%,
and $Ca(OH)_2$–62·1%, Ca_2SiO_4–25·6%, MgO–11·3%, H_2O—1·0%.

These results provide a basis for interpretation of the phase relationships in the more complex system CaO–MgO–SiO_2–CO_2–H_2O which have bearing on the petrogenetic relationships between kimberlites and carbonatites.

INTRODUCTION

THE field evidence that many carbonatites are intrusive and possibly magmatic was incompatible with available experimental data until WYLLIE and TUTTLE (1960) demonstrated that liquids in the system CaO–CO_2–H_2O precipitate calcite at temperatures down to 640°C through a wide pressure range. Liquids in this system were described as "synthetic carbonatite magmas". Systems more complex than CaO–CO_2–H_2O have been investigated in efforts to elucidate two problems: the physical and chemical nature of carbonatite magmas if they exist, and the origin of carbonatites. The second problem has been examined by studying the phase relationships in systems containing the "synthetic carbonatite magma" and silicate minerals occurring in rocks associated with carbonatites.

The increasing awareness in recent years of possible genetic connections between kimberlites and carbonatites (VON ECKERMANN, 1948, 1958; SAETHER, 1957; DAWSON, 1964; GARSON, 1962; DAVIDSON, 1964) led to the selection of forsterite and enstatite as suitable additional mineral components, giving sections through the five-component system CaO–MgO–SiO_2–CO_2–H_2O. It has been established in other systems such as CaO–SiO_2–CO_2–H_2O (HAAS and WYLLIE, 1963; WYLLIE and HAAS,

1965) that the phase behavior of portlandite, $Ca(OH)_2$, can be used as a guide to the phase behavior of compositions on the join $CaCO_3$–$Ca(OH)_2$. The phase relationships in the system CaO–MgO–SiO_2–H_2O, which are described in this paper, thus serve as a basis for interpretation of the phase relationships in the more complex system CaO–MgO–SiO_2–CO_2–H_2O (FRANZ, 1965), which will be described in a subsequent paper.

EXPERIMENTAL PROCEDURE

Starting materials

Commercial calcium hydroxide, magnesium oxide and silicic acid were used as source materials. These were prepared as described below, mixed in the desired proportions using a mechanical shaker (Wig-L-Bug Amalgamator), and stored in closed polyethylene vials within a desiccator containing NaOH and $CaSO_4$. *Calcium hydroxide:* A sample from a newly opened bottle of Fisher certified reagent was dried at 240°C for 2 hours. It was found that this gave optimum dehydration with minimum absorption of CO_2. *Magnesium oxide:* Fisher certified reagent was ignited at 1200°C for 1 hour. *Silica:* Matheson silicic acid ignited at 1200°C for 24 hours was used as a source of silica. *Forsterite:* synthetic forsterite was prepared by sintering the appropriate weight of MgO and silicic acid, and used instead of mechanical mixtures of MgO and SiO_2 in order to confirm that different starting materials yielded the same products. Mixtures were prepared on the two composition joins $Ca(OH)_2$–Mg_2SiO_4 and $Ca(OH)_2$–$MgSiO_3$, which will henceforth be referred to as the "forsterite join" and the "enstatite join", respectively. These joins are illustrated in Fig. 1 and 3, and the mixtures made up are shown by the runs in Fig. 4.

Equipment and method

The experimental techniques have been described in detail by WYLLIE and TUTTLE (1960). Samples of known composition were sealed within gold capsules and placed in cold-seal pressure vessels (TUTTLE, 1949). The pressure was raised to 1 kilobar and the pressure vessel and samples raised to the required temperature at constant pressure. The duration of runs varied from 1 hour to 40 days. The pressure vessels were quenched in compressed air with pressure maintained at 1 kilobar, and the temperature was reduced to below 100°C in 3 min. A few runs were quenched to a temperature below 100°C in less than 1 min by immersing the pressure vessel in cold water. No significant differences were noted between products obtained from the two quenching techniques. The samples were carefully removed from the gold capsule, and the phases present at the conditions of the run were determined from a combination of examination of the physical characteristics of the charge, petrographic observations of the crushed sample, and X-ray powder diffraction patterns. Temperature measurements were precise to ± 5°C, and the accuracy is believed to be better than ± 10°C. The precision of pressure measurements was ± 20 bars.

All reactions occurred rapidly, and there is good evidence that equilibrium was achieved. We assume that this was stable and not metastable. Runs varying in length from 1 hour to 40 days yielded consistent results. Runs on the join $Ca(OH)_2$–Mg_2SiO_4 made with different starting materials (synthetic forsterite or a mixture of MgO and SiO_2) yielded the same results. Reversibility was established by holding a sample at a selected temperature long enough to produce the phase assemblage characteristic for that temperature, and then lowering the temperature to a level where another phase assemblage should develop, and quenching the run after an hour or two. The lower-temperature assemblage developed with no evidence remaining for the former existence of the higher-temperature assemblage. The results obtained on the basis of the method of interpretation adopted are consistent with the phase rule, and they provide a consistent phase diagram.

Identification of phases

For convenience, the phases are identified by abbreviations. The phases encountered were: portlandite (CH), $Ca(OH)_2$; calciochondrodite (Ch), $Ca_5(SiO_4)_2(OH)_2$; dicalcium silicate (C_2S), Ca_2SiO_4; periclase (P), MgO; merwinite (Me), $Ca_3MgSi_2O_8$; liquid (L), with composition near

$Ca(OH)_2$; and vapor (V), with composition almost pure H_2O. The crystalline phases were identified by their optical properties, with X-ray diffraction patterns being used for occasional confirmation and to seek additional phases that might be overlooked in the optical examination. No solid solution was detected. The compositions of these phases and of others in the system are plotted in the quaternary tetrahedron of Fig. 1. The legends for Fig. 1 and 2 provide the key to the abbreviations for the additional phases plotted.

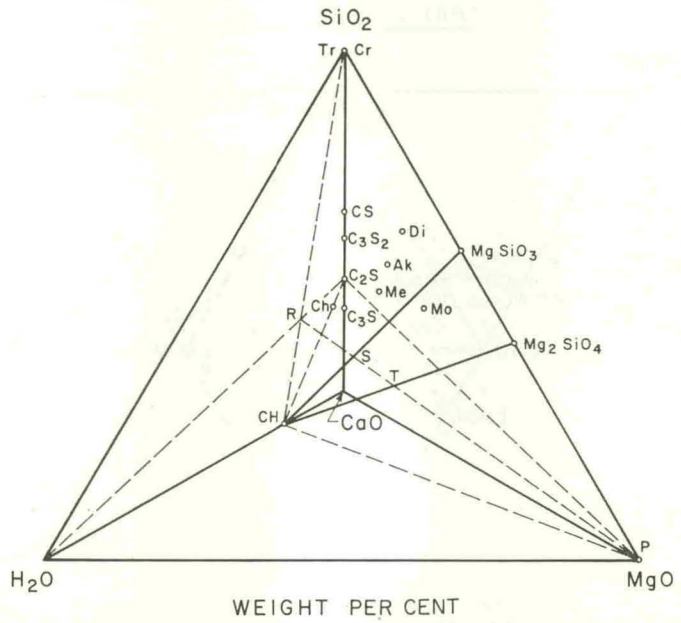

Fig. 1. Phases in the system CaO–MgO–SiO_2–H_2O. Abbreviations not explained in the text: Tr—tridymite, Cr—cristobalite, CS—wollastonite, C_3S_2—rankinite, C_3S—tricalcium silicate, Di—diopside, Ak—akermanite, Mo—monticellite. The composition triangle CH–MgO–SiO_2 contains the two joins investigated, $Ca(OH)_2$–Mg_2SiO_4 and $Ca(OH)_2$–$MgSiO_3$. This triangle intersects the upper face of the tetrahedron C_2S–CH–MgO–H_2O in the line RSTP.

The liquid could not be quenched to a glass, and former liquids were recognized by a combination of physical and microscopic characteristics of the samples, following the procedures described in detail by Wyllie and Tuttle (1960). Small spherical pits in the sample and on its surface were taken as evidence for the presence of a vapor phase in all runs containing a liquid phase. The diagnostic characteristics of portlandite, calciochondrodite and dicalcium silicate have been described by Wyllie and Tuttle (1960) or by Wyllie and Haas (1965). Primary periclase was easily identified by its octahedral habit, high refringence, and lack of birefringence. When quenched from the liquid, periclase formed minute specks in the quench portlandite. β-Ca_2SiO_4 and merwinite have rather similar optical properties, and X-ray diffractometer patterns were used to confirm their coexistence in one of the phase elements intersected (Fig. 4).

Previous Studies

The only previous study of the melting relationships in the quaternary system is Yoder's (1958) study of the effect of water vapor under pressure on the melting temperature of diopside. At a pressure of 1 kilobar on the join $CaMgSi_2O_6$–H_2O the melting temperature is about 1330°C, compared to 1390°C for diopside at 1 bar pressure. The amount of water dissolved in the liquid was not determined. By analogy with other silicate-water systems it is probably less than

5 wt.%. There is information available for the melting relationships in some of the bounding binary and ternary systems, and this is summarized in Fig. 2.

The relationships illustrated for the binary systems $CaO–SiO_2$, $CaO–H_2O$ and $SiO_2–H_2O$ are based on reviews by WYLLIE and HAAS (1965). with the temperatures for $CaO–H_2O$ being revised after HARKER (1964) and WYLLIE and RAYNOR (1965). The liquidus relationships for the system $CaO–MgO–SiO_2$ are from the revision by MUAN and OSBORN (1965, p. 92). Note that the

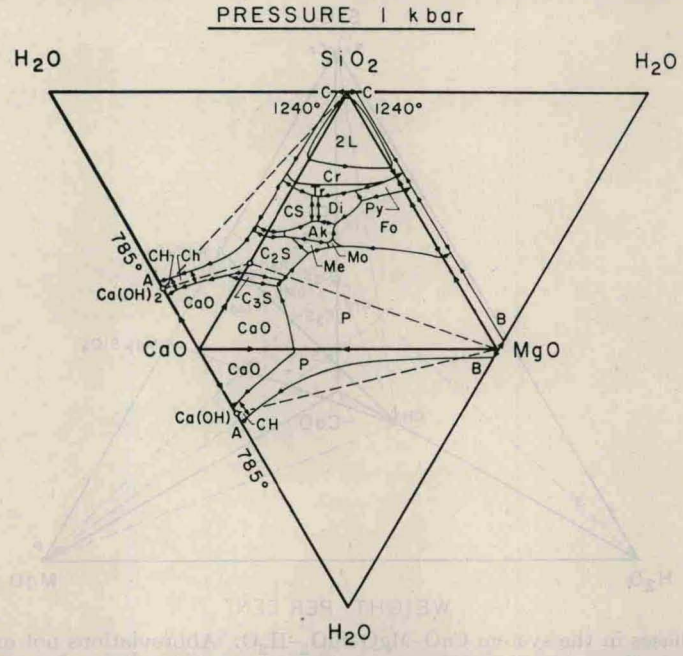

Fig. 2. The system $CaO–MgO–SiO_2–H_2O$ at 1 kilobar pressure: phase relationships for the four bounding ternary systems, in part schematic. For sources see text. Liquids on the boundaries AB, BC and AC are H_2O-saturated. The dashed lines are located in Fig. 1. Abbreviations not explained in the text or in Fig. 1: 2L—liquid miscibility gap, Py—pyroxene, Fo—forsterite.

dashed line $Ca_2SiO_4–MgO$ is a "thermal divide" over which liquids cannot cross during crystallization, equilibrium or fractional. The two field boundaries crossing the line (one binary and one ternary) pass through temperature maxima at the points of intersection. The probable phase relationships for the system $CaO–SiO_2–H_2O$ are taken from WYLLIE and HAAS (1965, Fig. 4), with the primary phase field for Ca_3SiO_5 being added. The probable phase relationships for the system $CaO–MgO–H_2O$ are adapted from Wyllie (1965a, Fig. 2). The liquidus phase relationships for the system $MgO–SiO_2–H_2O$ are schematic; the solubility of H_2O in the liquid phase of the system $SiO_2–H_2O$ at 1 kilobar pressure is 3·8 wt.% (KENNEDY *et al.*, 1962), and it is assumed that about the same amount of H_2O dissolves in all silicate liquids of the system $MgO–SiO_2$ at this pressure. It is also assumed, for convenience of representation, that the two-liquid field extending from the binary system terminates in a critical point at a liquid composition which is unsaturated with respect to H_2O. A similar assumption had been made in the system $CaO–SiO_2–H_2O$ (WYLLIE and HAAS, 1965).

THE VAPOR-SATURATED LIQUIDUS SURFACE

A liquidus is defined as the locus of liquids that are just saturated with respect to crystals at a specified pressure. In an isobaric ternary system a liquidus is

divariant and may be represented as a surface in a TX prism. For silicate systems containing a volatile component such as H_2O, a liquidus surface may be terminated by an isobaric field boundary giving the locus of liquids that are saturated with respect to two phases, one crystalline, and one a vapor phase; this is a vapor-saturated field boundary. The H_2O-saturated field boundaries in each of the ternary systems CaO–MgO—H_2O, CaO–SiO_2–H_2O, and MgO–SiO_2–H_2O are AB, AC, and BC, respectively (Fig. 2). The liquidus field boundaries of ternary systems extend into quaternary tetrahedra as isobaric divariant surfaces; the ternary field boundaries

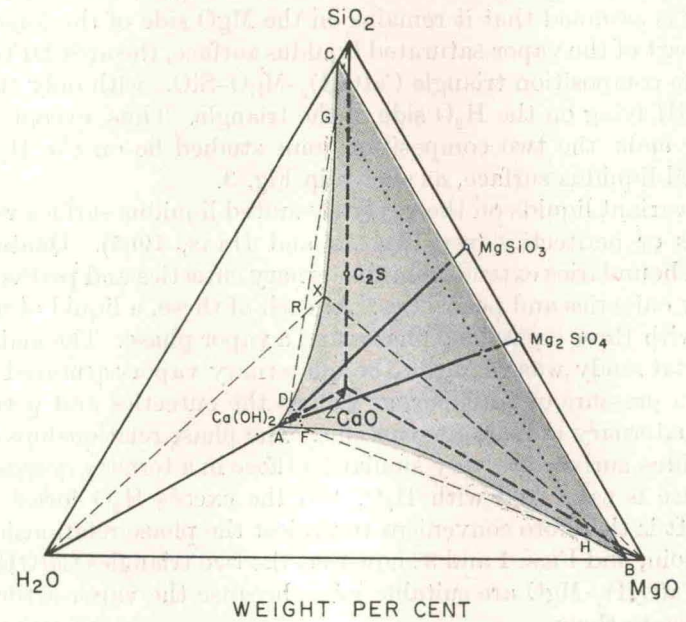

Fig. 3. The vapor-saturated liquidus surface ABC (shaded) connecting the ternary vapor-saturated liquidus field boundaries AB, BC, and AC shown in Fig. 2. The composition triangle $Ca(OH)_2$–MgO–SiO_2 intersects the shaded surface along the dotted lines DF and GH. The upper face of the compatibility tetrahedron C_2S–$Ca(OH)_2$–MgO–H_2O intersects the shaded surface along the dashed line XB, which is therefore a thermal maximum on the surface.

AB, AC, and BC in Fig. 2 form the edges of the quaternary vapor-saturated liquidus surface shown schematically in Fig. 3. The approximate position of the shaded surface ABC can be ascertained from Figs. 1 and 2. The vapor-saturated liquidus surface is *not* a normal liquidus surface; the characteristics of such a surface have been discussed by Wyllie and Haas (1965).

The dashed lines in Fig. 1 delineate the composition triangle $Ca(OH)_2$–MgO–SiO_2, which includes the two composition joins studied, and the tetrahedron Ca_2SiO_4–$Ca(OH)_2$–MgO–H_2O. The dashed lines can also be located in Fig. 2. The composition triangle intersects the upper face of this tetrahedron in the line RSTP (Fig. 1), with S and T lying on the enstatite and forsterite joins, respectively. The composition triangle also intersects the ternary field boundaries in the points

D, F, G and H, as shown in Fig. 3, and it intersects the quaternary surface ABC along the dotted lines DF and GH. The positions of the lines are only estimated, but there is little possibility of variation from the plotted positions. The upper surface of the Ca_2SiO_4–$Ca(OH)_2$–MgO–H_2O tetrahedron, Ca_2SiO_4–MgO–H_2O, intersects the vapor-saturated liquidus surface in the dashed line XB in Fig. 3. The line XB is a thermal divide on the vapor-saturated liquidus surface, corresponding to the thermal divide Ca_2SiO_2–MgO of the anhydrous system (Fig. 2) in the presence of excess H_2O vapor. The line of intersection of the vapor-saturated liquidus surface with the triangle Ca_2SiO_4–$Ca(OH)_2$–MgO is not illustrated in Fig. 3. It would extend from F to H, and it is assumed that it remains on the MgO side of the forsterite join.

The main part of the vapor-saturated liquidus surface, the area DFGH, lies on the CaO side of the composition triangle $Ca(OH)_2$–MgO–SiO_2, with only the small areas ADF and BCGH lying on the H_2O side of the triangle. Thus, except for small portions at either ends, the two composition joins studied lie on the H_2O side of the vapor-saturated liquidus surface, as shown in Fig. 3.

Isobaric invariant liquids on the vapor-saturated liquidus surface will be referred to as eutectics or peritectics (see WYLLIE and HAAS, 1965). Quaternary vapor-saturated field boundaries extend from the ternary eutectics and peritectics and meet at quarternary eutectics and peritectics. At each of these, a liquid of fixed composition coexists with three crystalline phases and a vapor phase. The main objective of the experimental study was to locate the quaternary vapor-saturated liquidus field boundaries at a pressure of 1 kilobar, as well as the eutectics and peritectics corresponding to quaternary univariant reactions. The phase relationships on the vapor-saturated liquidus surface are very similar to those in a ternary system, except that the liquid phase is saturated with H_2O, and the excess H_2O forms as additional vapor phase. It is therefore convenient to project the phase relationships from H_2O onto a planar join, and Figs. 1 and 3 show that the two triangles $Ca(OH)_2$–MgO–SiO_2 and Ca_2SiO_4-$Ca(OH)_2$–MgO are suitable joins, because the vapor-saturated liquidus surface lies close to them.

EXPERIMENTAL RESULTS

Phase fields intersected

Figure 4 illustrates the phase fields intersected at 1 kilobar pressure in the temperature range 700–900°C by parts of the enstatite join and the forsterite join. The positions of critical runs are plotted, and appropriate details are listed in Table 1. The criteria for the recognition of a trace of vapor in the small samples that we employed are not unambiguous, but there is evidence for the presence of vapor in all runs completed. This is consistent with the estimated position of the vapor-saturated liquidus surface in Fig. 3.

On the $Ca(OH)_2$ side of the compositions S and T (Figs. 1 and 4), five four-phase elements are intersected by the enstatite and forsterite joins, with a sixth being required by the phase relationships in the enstatite join. In each join, these are arranged around two isothermal lines representing isobaric invariant reactions:

$$\text{a eutectic at } 725°\text{C, CH} + \text{Ch} + \text{P} + \text{V} \rightleftharpoons \text{L}(W_1)$$

$$\text{a peritectic at } 875°\text{C, Ch} + \text{P} + \text{V} \rightleftharpoons \text{C}_2\text{S} + \text{L}(W_2).$$

Table 1. Quench runs in the system CaO–MgO–SiO_2–H_2O at 1 kilobar pressure

Abbreviations: CH—$Ca(OH)_2$; Ch—$Ca_5(SiO_4)_2(OH)_2$; C_2S—Ca_2SiO_4; P—MgO; Me—$Ca_3MgSi_2O_8$; L—liquid; V—vapor; tr—trace

Composition Wt.% CH	Temp. (°C)	Time in days or hours	Interpreted phase assemblage
(a) Join $Ca(OH)_2$–Mg_2SiO_4			
95	715	17 dy	CH + Ch + P + V
95	725	18 hr	CH + Ch + P + L + V
95	730	24 hr	Ch + P + L + V
95	785	24 hr	Ch + trP + L + V
95	810	18 hr	Ch + L + V
95	825	4 dy	L + V
95	830	10 dy	L + V
90	715	17 dy	CH + Ch + P + V
90	725	18 hr	CH + Ch + P + trL + V
90	730	24 hr	Ch + P + L + V
90	755	4 dy	Ch + P + L + V
90	765	18 hr	Ch + P + L + V
90	835	5 dy	Ch + P + L + V
90	850	19 hr	trCh + P + L + V
90	870	24 hr	P + L + V
90	900	6 hr	L + V
85	715	17 dy	CH + Ch + P + V
85	725	18 hr	CH + Ch + P + L + V
85	850	19 hr	Ch + P + L + V
85	870	24 hr	trCh + P + L + V
85	885	3 dy	P + L + V
80	715	17 dy	CH + Ch + P + V
80	725	18 hr	CH + Ch + P + L + V
80	730	24 hr	Ch + P + L + V
80	870	24 hr	Ch + C_2S + P + L + V
80	885	24 hr	P + L + V
80	950	6 hr	P + L + V
70	715	17 dy	CH + Ch + P + V
70	755	4 dy	Ch + P + L + V
70	780	10 dy	Ch + P + L + V
70	830	10 dy	Ch + P + L + V
70	885	24 hr	C_2S + P + L + V
70	950	6 hr	C_2S + P + L + V
60	715	17 dy	CH + Ch + P + V
60	785	10 dy	Ch + P + L + V
60	830	10 dy	Ch + P + L + V
60	885	3 dy	C_2S + P + L + V
60	950	6 hr	C_2S + P + L + V
(b) Join $Ca(OH)_2$–$MgSiO_3$			
95	720	40 dy	CH + Ch + P + L + V
95	735	7 dy	CH + Ch + L + V
95	755	7 dy	CH + Ch + L + V
95	770	25 hr	trCh + L + V
95	790	24 hr	L + V
85	720	40 dy	CH + Ch + P + trL + V

Table 1 (*cont.*)

Composition Wt.% CH	Temp. (°C)	Time in days or hours	Interpreted phase assemblage
(b) Join $Ca(OH)_2$–$MgSiO_3$			
85	735	7 dy	Ch + P + L + V
85	800	1½ dy	Ch + P + L + V
85	825	22 hr	Ch + L + V
85	885	24 hr	Ch + L + V
85	895	1 hr	trCh + trC_2S + L + V
85	930	1 hr	L + V
77·5	870	24 hr	Ch + P + L + V
77·5	885	24 hr	C_2S + P + L + V
77·5	900	1 hr	C_2S + L + V
70	720	40 dy	trCH + Ch + P + L + V
70	735	7 dy	Ch + P + trL + V
70	850	2½ dy	Ch + P + L + V
70	885	3 dy	C_2S + P + L + V
70	930	1 hr	C_2S + P + L + V
55	800	1½ dy	Me + C_2S + P + V
55	850	2½ dy	Me + C_2S + P + V
55	930	1 hr	Me + C_2S + P + V

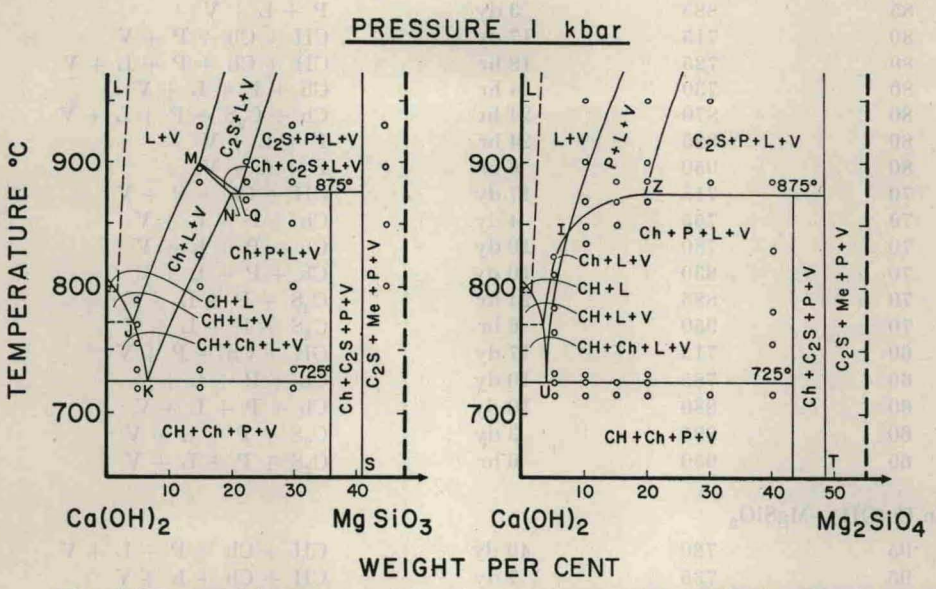

Fig. 4. Phase fields intersected by the composition join $Ca(OH)_2$–$MgSiO_3$ and $Ca(OH)_2$–Mg_2SiO_4 at 1 kilobar pressure. For abbreviations see text.

The latter equation assumes that the liquid composition, W_2 lies on the H_2O side of the triangle Ca_2SiO_4–$Ca(OH_2)$–MgO. If it lies on the CaO side of the triangle then the vapor phase would occur on the right hand side of the equation.

The boundaries between the fields for L + V and the three-phase elements in Fig. 4 correspond to sections through the vapor-saturated liquidus surface, projected onto these composition joins along the tie-lines connecting the liquid compositions to H_2O. The points J, M and I on the boundary of the L + V field in Fig. 4 correspond to points on the vapor-saturated liquidus field boundaries. The point J separates the primary crystallization of CH from that of Ch (in the presence of H_2O vapor), M separates the primary fields of Ch and C_2S, and I separates the primary fields of Ch and P. The four-phase elements appropriate for each of these field boundaries are intersected in areas extending from these points in Fig. 4.

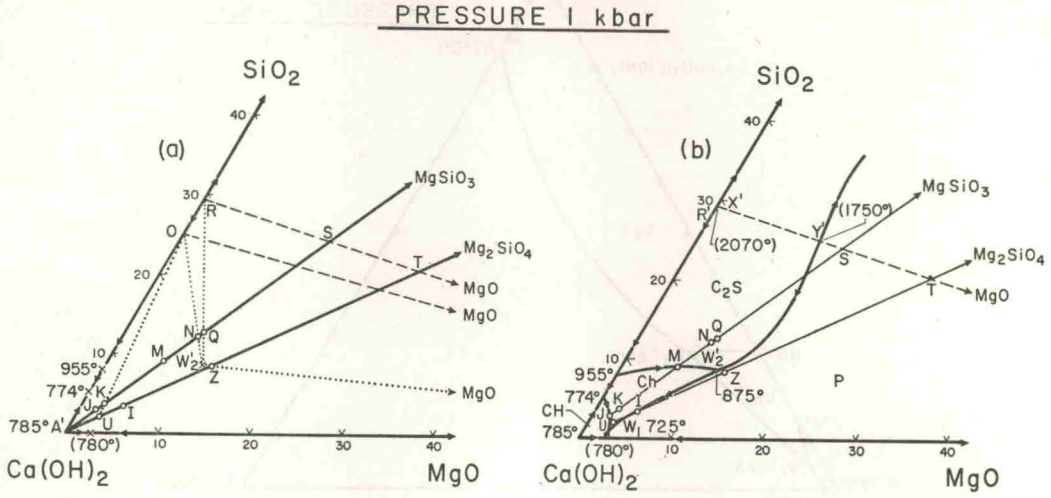

Fig. 5. Phase relationships on the vapor-saturated liquidus surface when projected onto the triangle $Ca(OH)_2$–MgO–SiO_2, as constructed from the experimental results in Fig. 4. Note the line RST MgO in Figs. 1 and 3.

(a) The composition joins, the construction points plotted in Fig. 4, and the dotted construction lines. See text for details.

(b) Positions of vapor-saturated field boundaries determined from Fig. 4(a). The temperatures in parentheses are estimated. See text for more details.

Vapor-saturated liquidus surface

The arrangement of primary phase fields and field boundaries illustrated in Fig. 5(b) corresponds to a projection of the vapor-saturated liquidus surface onto the composition triangle $Ca(OH)_2$–MgO–SiO_2 along the liquid-H_2O tie-lines; the projection was from the surface towards H_2O, except for the small area ADF of Fig. 3. The projection was constructed from what is known of the bounding ternary systems (Fig. 2) and from the experimentally located phase fields of Fig. 4; the measured points from Fig. 4, and the construction lines, are illustrated in Fig. 5(a).

In Fig. 5(a), the dashed line RST is the upper limit of the Ca_2SiO_4–$Ca(OH)_2$–MgO–H_2O tetrahedron (compare Fig. 1). The point of intersection of the lines Ch–H_2O and CH–R in Fig. 1 is represented by point O in Fig. 5(a). The crosses on the sides $Ca(OH)_2$–SiO_2 and $Ca(OH)_2$–MgO

represent the ternary vapor-saturated eutectics and peritectics (Fig. 2). The points J, K, M, N and Q, and U, I and Z located in Fig. 4. J, M and I have already been described as points on the field boundaries and they are so plotted in Fig. 5(b). The other points permit location of the liquid compositions for the projected peritectic (W_2') and eutectic (W_1').

W_2' in Fig. 5 is the point of intersection of the L(W_2)-V line of the five-phase tie figure C_2S + Ch + P + L + V with the composition triangle $Ca(OH)_2$–MgO–SiO_2. In Fig. 5(a), the dotted lines ON extended and RQ extended, are the intersections of sides of the four-phase element Ch + C_2S + L + V (Fig. 4a), which must meet at the point W_2'. Similarly, the dotted lines RQ extended and MgO–Z extended are the intersections of two sides of the four-phase element C_2S + P + L + V (Figs. 4a and 4b), and these must also meet at W_2'. The point of intersection of the dotted lines ON, RQ and MgO–Z is therefore the projected peritectic liquid W'_2.

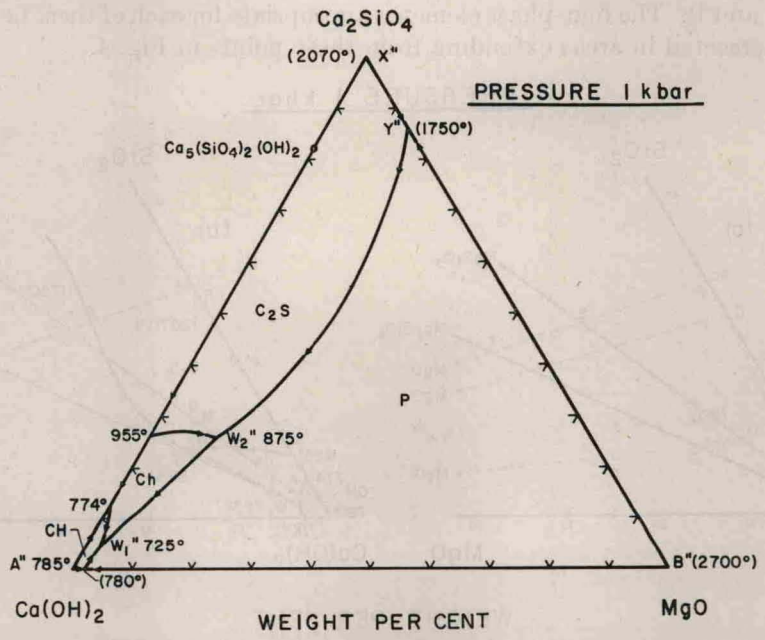

Fig. 6. Phase relationships on the vapor-saturated liquidus surface when projected onto the triangle $Ca(OH)_2$–Ca_2SiO_4–MgO, as calculated from Fig. 5(b). Temperatures in parentheses are estimated. For abbreviations see text.

W_1' in Fig. 5 is the point of intersection of the L(W_1)-V line of the five-phase tie-figure CH + Ch + P + L + V with the plane $Ca(OH)_2$–MgO–SiO_2. The dotted line OKU extended is the line of intersection of the plane Ch + L + V, which forms part of the five-phase tie-figure. and W_1' therefore lies on this line. The limits placed on the locations of the projected field boundaries by the various construction points (Fig. 5b) locate the projected eutectic liquid, W_1', at a point very close to U.

The projected vapor-saturated liquidus surface illustrated in Fig. 5(b) was constructed from the information on summarized in Fig. 4 and 5(a). The field boundaries separate the fields for the primary crystallization (in the presence of H_2O vapor) of CH, Ch, P and C_2S. The dashed line X′Y′-MgO shows the projection of the line XB in Fig. 3, and this coincides with the line RST (compare Figs. 1, 3 and 5(b).

The compositions of the projected liquids W_2' and W_1' were measured on Fig. 5(b) and recalculated in terms of the apices of the tetrahedron Ca_2SiO_4–$Ca(OH)_2$–MgO–H_2O. By omitting H_2O and recalculating to 100 per cent the positions of the liquids W_2 and W_1 when projected from H_2O onto the triangle Ca_2SiO_4–$Ca(OH)_2$–MgO were obtained. These have been plotted

with double superscripts in Fig. 6, and the projected field boundaries around them were sketched from Fig. 5(b) and the known ternary relationships. Figure 6 is thus a projection of the vapor-saturated liquidus surface onto the plane Ca_2SiO_4–$Ca(OH)_2$–MgO along the H_2O-liquid tie-lines. Figure 3 indicates that the part of the vapor-saturated liquidus surface within the area AW_1W_2YX (compare Figs. 3 and 6) is situated just a short distance on the H_2O side of this triangle. The arrangement of quaternary field boundaries shown in Fig. 6 is thus a more accurate representation than Fig. 5(b) of the phase relationships on the vapor-saturated liquidus surface within the tetrahedron CaO–Ca_2SiO_4–MgO–H_2O. This projection has the added advantage that all of the crystalline phases encountered at this pressure have compositions lying on the plane. Figure 6, summarizing the results obtained in this study, has been combined with other known and inferred data to provide Fig. 7.

The compositions of the projected liquids are:

W_2'': $Ca(OH)_2$—62·7%, Ca_2SiO_4—25·9%, MgO—11·4%,
W_1'': $Ca(OH)_2$—93·2%, Ca_2SiO_4—4·3%, MgO—2·5%.

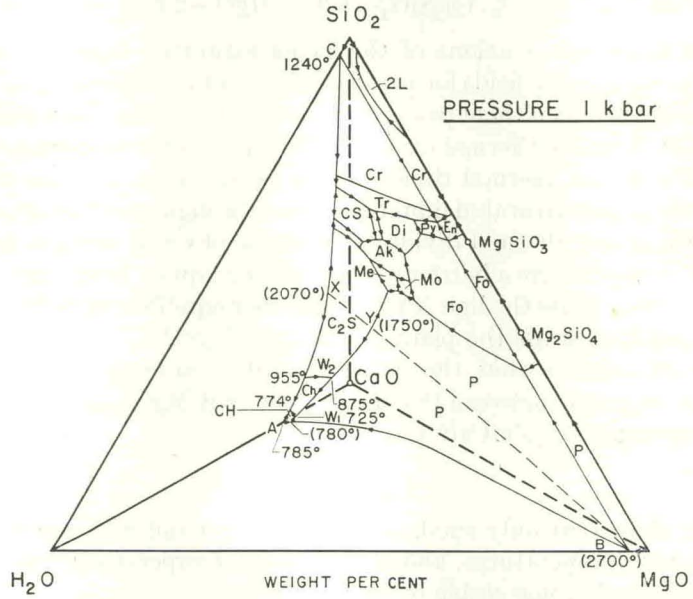

Fig. 7. The system CaO–MgO–SiO_2–H_2O at 1 kilobar pressure: schematic diagram based on Figs. 2, 3 and 6. The phase relationships for the system MgO–SiO_2–H_2O are shown, see Fig. 2; En—enstatite. ABC is the vapor-saturated liquidus surface transferred from Fig. 3, and the dashed line XYB is a thermal maximum on this surface. The phase relationships above XYB are based on the system CaO–MgO–SiO_2 (see Fig. 2), and those below XYB are based on the experimental results shown in Fig. 6. Temperatures in parentheses are estimated. For abbreviations see text or legends for Figs. 1 and 2.

It is convenient to consider the vapor-saturated liquidus surface in two portions, above and below the thermal divide XB shown in Figs. 3 and 7. The phase relationships above the line XYB in Fig. 7 are assumed to be similar to those of the anhydrous system (Fig. 2), with temperatures somewhat lowered as a result of the small percentage of H_2O dissolved in the liquids, and with the two-liquid volume being closed before the liquids become saturated with H_2O. This part of the vapor-saturated

liquidus surface remains very close to the anhydrous base, and the distribution of isotherms on the anhydrous liquidus surface permits a confident statement that primary fields for dicalcium silicate and for periclase are the only ones extending across XYB on the vapor-saturated liquidus surface, through a wide pressure range. The phase relationships below the line XYB in Fig. 7 are more complex than in the anhydrous system, because of the formation of hydrous compounds with stability fields on the liquidus. The surface here extends somewhat towards the H_2O corner of the quaternary tetrahedron. The liquid compositions W_2 and W_1 are believed to contain a little more H_2O than the projected liquids W_2'' and W_1'' in Fig. 6, and making adjustments to allow for this, the estimated compositions of the quaternary peritectic and eutectic liquids are:

W_2: $Ca(OH)_2$—62·1%, Ca_2SiO_4—25·6%, MgO—11·3%, H_2O—1·0%.
W_1: $Ca(OH)_2$—92·7%, Ca_2SiO_4—4·3%, MgO—2·5%, H_2O—0·5%.

The upper and lower portions of the vapor-saturated liquidus surface have in common the primary phase fields for periclase (P) and for dicalcium silicate (C_2S), and the field boundary between them passes through a pronounced maximum in temperature at the point Y on the thermal divide XYB. All available evidence suggests that the portion XY of the thermal divide would persist as a significant temperature maximum on the vapor-saturated liquidus surface through a very wide pressure range. The portion YB of the thermal divide, although a physical temperature maximum only near to Y, is as effective a barrier to crystallizing liquids as the thermal maximum XY. Liquids cannot cross the line XYB with either equilibrium or fractional crystallization; nor can they cross the plane XYB.MgO.Ca_2SiO_4.

These results indicate that the vapor-saturated eutectic liquid in the system CaO–MgO–H_2O contains between 0·5 and 3·5 per cent MgO, and probably less than 1% H_2O in excess of the join $Ca(OH)_2$–MgO.

DISCUSSION

The results show that only small amounts of MgO and SiO_2 are soluble in fused portlandite at low temperatures, and that liquidus temperatures rise sharply when periclase or silicates become stable on the liquidus.

The existence of the thermal divide XYB on the vapor-saturated liquidus surface shows that, with fractional crystallization at this pressure, the high temperature silicate liquids with compositions richer in SiO_2 than XYB are unable to yield a low temperature residual melt that is capable of precipitating the hydrated phases. Crystallization of these minerals yields only silicates and a separate vapor phase. Any liquid with composition poorer in SiO_2 than XYB, however, will yield a hydrated low temperature residual liquid with fractional crystallization, and this liquid will precipitate hydrated phases. A similar thermal divide was encountered in the system CaO–SiO_2–CO_2–H_2O (WYLLIE and HAAS, 1965). Increasing pressure is not likely to cause any significant changes in the position or stability of the thermal divide until different mineral assemblages are produced at very high pressures, perhaps in the 15 to 30 kb range.

Figure 7 can be used as a model for the system CaO–MgO–SiO_2–CO_2. From what is known of the system CaO–SiO_2–CO_2–H_2O (WYLLIE and HAAS, 1965), it is to be

anticipated that the position of the vapor-saturated liquidus surface would be rather similar with $CaCO_3$ instead of $Ca(OH)_2$, and spurrite instead of calciochondrite. Liquidus temperatures would be somewhat higher throughout the system, because CO_2 is less soluble in these liquids than H_2O, and calcite in the presence of CO_2 melts at 1310°C instead of 785°C for portlandite in the presence of H_2O. The thermal divide corresponding to XYB should persist in the CO_2 system. It may therefore be concluded that liquids with compositions richer in SiO_2 than XYB in Fig. 7 with CO_2 as an additional component, are unable to yield low temperature residual liquids by fractional crystallization, and these liquids are therefore unable to precipitate carbonated and hydrated phases. Only liquids with compositions poorer in SiO_2 than XYB are capable of yielding through fractional crystallization residual liquids that precipitate carbonated and hydrated phases.

The high temperature silicate liquids that precipitate forsterite, pyroxenes, and monticellite may be compared with ultrabasic magmas, and the low temperature hydrated or carbonated liquids may be used as a model for carbonatite magmas. The results presented in this paper thus indicate that normal peridotite or kimberlite magmas (if these exist in nature) are incapable of producing a carbonatite magma as a residue from fractional crystallization.

When CO_2 replaces H_2O as a component, complexities arise involving the decarbonation reactions. Intersection of the decarbonation reactions involving silicate minerals such as forsterite and monticellite with the melting reactions will permit these minerals to crystallize in two different environments: on the SiO_2 side of the thermal divide XYB, as shown in Fig. 7, and also on the low temperature side of this thermal barrier, alongside calcite. This introduces all kinds of additional possibilities (FRANZ, 1965). Finally, it must be mentioned that the presence of alkalis in the system may modify the paths of crystallization considerably (WYLLIE, 1965), and a liquid corresponding to an alkali peridotite magma may be able to bypass the thermal divide XYB and yield a carbonated residual liquid by fractional crystallization.

Acknowledgements—We would like to thank D. M. ROY for her assistance at various stages during the work, W. C. LUTH for a critical review of the manuscript, and the National Science Foundation for supporting the research at the Pennsylvania State University with Grants G-19588 and GP-1870.

REFERENCES

DAVIDSON C. F. (1964) On diamantiferous diatremes. *Econ. Geol.* **59,** 1368–1380.

DAWSON J. B. (1964) Carbonate tuff cones in northern Tanganyika. *Geol. Mag.* **101,** 129–137.

ECKERMANN H. VON (1948) The alkaline district of Alno Island. *Sverig. geol. Unders. Ser. Ca,* No. 36.

ECKERMANN H. VON (1958) The alkaline and carbonatitic dykes of the Alno formation on the mainland northwest of Alno island. *Kungl. Svensk. Vetrnskap., Handl., Fj. ser., Bd.* **7,** 61 p.

FRANZ G. W. (1965) Melting relationships in the system $CaO–MgO–SiO_2–CO_2–H_2O$: a study of synthetic kimberlites. Ph. D. thesis, The Pennsylvania State University.

GARSON M. S. (1962) The Tundulu carbonatite ring-complex in southern Nyasaland. *Geol. Survey Nyasaland, Mem.* **2,** 248 p.

HAAS J. L. and WYLLIE P. J. (1963) The system $CaO–SiO_2–CO_2–H_2O$. 1. Melting relationships in the presence of excess vapor (abstract). *Trans. Amer. Geophys. Un.* **44,** 117.

HARKER R. I. (1964) Differential thermal analysis in closed systems at high hydrostatic pressures. *Amer. Min.* **49,** 1741–1747.

Kennedy G. C., Wasserburg G. J., Heard H. C. and Newton R. C. (1962) The upper three-phase region in the system SiO_2–H_2O. *Amer. J. Sci.* **260,** 501–521.

Muan A. and Osborn E. F. (1965) *Phase Equilibria among Oxides in Steelmaking.* Addison-Wesley, Reading, Mass.

Saether E. (1957) The alkaline district of the Fen area in southern Norway. *Norsk. Vidensk. Selsk. Skrift* **1.**

Tuttle O. F. (1949) Two pressure vessels for silicate-water studies. *Bull. Geol. Soc. Amer.* **60,** 1727–1729.

Wyllie P. J. (1965a) Melting relationships in the system CaO–MgO–CO_2–H_2O, with petrological applications. *J. Petrol.* **6,** 101–123.

Wyllie P. J. (1965b) Experimental data bearing on the petrogenetic links between kimberlites and carbonatites. Proc. Int. Miner. Assoc., New Delhi, 1964. *Indian Min.*, in press.

Wyllie P. J. and Haas J. L. (1965) The system CaO–SiO_2–CO_2–H_2O: 1. Melting relationships with excess vapor at 1 kilobar pressure. *Geochim. et Cosmochim. Acta* **29,** 871–892.

Wyllie P. J. and Raynor E. J. (1965) D.T.A. and quenching methods in the system CaO–CO_2–H_2O. *Amer. Min.*, in press.

Wyllie P. J. and Tuttle O. F. (1960) The system CaO–CO_2–H_2O and the origin of carbonatites. *J. Petrol.* **1,** 1–46.

Yoder H. S. (1958) Effect of water on the melting of silcates. *Carnegie Inst. Wash. Y. B.* **57,** 189–191.